

COMSTAR Spacecraft Product-of-Inertia Coupled Electronic Nutation Damper

Loren I. Slafer* and John W. Smay†
Hughes Aircraft Company, El Segundo, Calif.

The design and flight performance of an innovative scheme for active nutation control flown on the COMSTAR spacecraft is described. This spacecraft is a dual-spin configuration stabilized in a maximum energy state spinning about an axis of minimum inertia. The damping mechanization implemented employs a rotor-mounted accelerometer for sensing and the despin motor as actuator, applying transverse axis damping torques through the despun product of inertia. Significant advantages of the scheme are that a broadly tuned damper, insensitive to parameter uncertainties, is provided with very low hardware weight, complexity and cost.

Nomenclature

$F_1(s), F_2(s)$	= nutation rate feedback filters operating on signal in rotor and platform coordinates, respectively
$H(j\lambda_n)$	= $\beta e^{j\theta}$
$H(s)$	= payload pointing loop open-loop transmission (excluding nutation dipole)
I_{13}	= platform product of inertia
I_p, I_s	= platform and rotor spin moments of inertia, respectively
I_T	= total vehicle transverse moment of inertia
K_1, K_2, K	= nutation rate feedback gains
K_n	= $Kr(2 - \sigma)I_{13}/I_sI_p$ = normalized transverse rate feedback gain
$L(s)$	= system open-loop transmission matrix
$P(s)$	= plant matrix of vehicle dynamics
$Q(s)$	= open-loop nutation dipole
r	= I_{13}^2/I_TI_p
r_0	= transverse component of radius vector from vehicle c.m. to accelerometer
σ	= inertia ratio, I_s/I_T
ω_p, ω_s	= nominal platform and rotor inertial angular rate about the spin axis
ω_r	= $\omega_s - \omega_p$ = relative angular rate
λ_n, Ω_n	= open-loop nutation frequencies in platform and rotor coordinates, respectively
ω	= $[\omega_1, \omega_2, \omega_3]^T$ = perturbation about nominal of platform rate in platform coordinates
ϕ	= total phase shift in accelerometer transverse rate feedback path
ω_{s1}, ω_{s2}	= ω_1, ω_2 in rotor coordinates
θ_p	= platform inertial phase (small transverse angle approximation)
$\psi = \omega_r t$	= relative spin phase of rotor and platform
θ_n	= nutation half-angle magnitude (small angles)
τ_d	= active nutation damping time constant
τ_n	= $2/(r\lambda_n)$ = normalized nutation damping time constant

I. Introduction

THE COMSTAR satellite is a geosynchronous domestic communications satellite. Two spacecraft have been

launched and are currently in operation carrying communication traffic across the United States and with Alaska and Hawaii. The satellite utilizes a dual-spin configuration in which a spinning rotor provides basic gyroscopic attitude rigidity, with a despun platform providing continuous Earth-pointing of the communications antennas. This paper describes the design, implementation, and flight performance of a unique active nutation stabilization scheme developed for the COMSTAR satellite.

The general stability criteria for dual-spin spacecraft are well known and will not be repeated here. Detailed discussions of stability can be found in Refs. 1-4. For the COMSTAR spacecraft, with a spin-to-transverse inertia ratio ranging between 0.22 and 0.28 over the mission, the destabilizing effects of fuel slosh produce a minimum nutation divergence time constant of ~ 70 s at the worst-case propellant loading condition. In addition, during transfer orbit operations, kinematic nutation coupling through the attitude sensors and pointing control system could generate destabilizing time constants as low as 40 s at the worst-case spacecraft attitude.

Passive mechanical dampers, mounted on the despun platform, were initially employed on COMSTAR to provide the despun energy dissipation necessary for asymptotic nutation stability. These dampers have a successful flight history on the INTELSAT IV and IVA vehicles, but have inherent weight penalties and response limitations. In order to provide additional stability margins and operational flexibility, the active nutation damping scheme presented in this paper was developed. The active damper, using inherent dynamic coupling and the existing control system elements, alleviated the problems associated with the passive dampers with minimal added complexity and weight and provided significant performance improvements.

For a spacecraft configuration in which the despun payload possesses a product of inertia (POI) between the spin and transverse axes, it has been shown⁵⁻⁸ that nutation can be controlled actively onboard through the use of properly generated control torques about the spin axis. Reference 8 presented a closed-form expression for the resulting closed-loop nutation damping time constant.

Use of the payload pointing control system for active nutation control to augment the passive dampers via the POI dynamic coupling was shown⁸ to have fundamental limitations on the strength of the achievable nutation damping. These limitations are imposed by the combined effects of the required control system stability margins, and the ratio of the POI to both the total vehicle transverse moment of inertia (MOI) and payload MOI about the spin axis. As the magnitude of the POI is reduced relative to the platform spin and vehicle transverse inertias, the resulting active nutation damping becomes less effective with no compensation achievable through modification of the control system design.

Received July 13, 1977; presented as Paper 77-1056 at the AIAA 1977 Guidance and Control Conference, Hollywood, Fla., Aug. 8-10, 1977; revision received Dec. 19, 1977. Copyright © American Institute of Aeronautics and Astronautics, Inc., 1977. All rights reserved.

Index category: Spacecraft Dynamics and Control.

*Senior Staff Engineer, Guidance and Control Systems Laboratory, Space and Communications Group, Member AIAA.

†Section Head, Guidance and Control Systems Laboratory, Space and Communications Group, Member AIAA.

The active nutation damper treated herein (described in detail in Ref. 9) uses the despin motor and despun product of inertia together to form an actuator to apply transverse axis damping torques, but employs a separate nutation sensor rather than relying upon the pointing control loop sensing, with its attendant constraints. Nutation is sensed by a rotor-mounted accelerometer and processed for application as a torque command to the despin motor. This separate sensing path largely removes the constraints of the pointing control design and permits realization of a very effective and broadly tuned damper loop. The accelerometer sensor is necessary for a large angle thruster actuated damping loop,¹⁰ thus no sensors are added by the despin damping loop. The only additional hardware required to implement the damping loop is a minimal amount of processing electronics.

This paper describes the experience gained in applying this active damping technique to a flight vehicle. Section II describes in functional terms the COMSTAR attitude stabilization and pointing control systems. A summary of the dynamic equations applicable to the damping system design and the COMSTAR active damper performance characteristics are summarized in Sec. III. Flight performance data from COMSTAR are presented and discussed in Sec. IV.

II. COMSTAR Attitude and Despin Control Subsystem

The fundamental design of the COMSTAR spacecraft is based on a spinning rotor which contains most of the utility subsystems (power, propulsion, attitude and despin control, and a portion of the telemetry and command subsystem), and a large despun, Earth-oriented platform containing the communications payload and the remaining portion of the telemetry and command subsystem. The Attitude and Despin Control Subsystem (ADCS), shown functionally in Fig. 1, performs four primary functions, 1) provides the rotating mechanical interface between spinning and despun sections of the spacecraft, 2) provides for transfer of both electrical power and telemetry and command signals across the interface, 3) provides automatic despin, acquisition, and Earth tracking of the communications platform, and 4) provides measurement, control, and stabilization of the rotor spin vector attitude.

The attitude control functions are divided into two basic categories: spin axis attitude control and stabilization and despin pointing control. Inertial orientation of the spacecraft spin axis is achieved via ground-commanded firing of the axial thrusters based on attitude data derived from the outputs of spinning Earth and Sun sensors. By firing one axial thruster in a pulsed mode at the proper rotor spin phase, the spin axis of the vehicle can be rotated in inertial space and set in any desired orientation. Because COMSTAR operates normally in an inherently unstable configuration (i.e., spinning about an axis of minimum inertia) energy dissipation on the despun platform is required for passive asymptotic attitude stability. At the inception of the COMSTAR program, this function was implemented with the inclusion of two passive mechanical eddy-current dampers mounted to the upper portion of the despun platform antenna support structure. These dampers are simple mechanical oscillators tuned to a specific frequency and are excited by nonzero transverse vehicle rates (nutation). Operating at its resonant frequency, a single COMSTAR damper provides a nutation transient decay time constant (in the absence of any destabilizing influence) of 45 s (25s for both dampers) over a linear range of 0.25 deg of nutation. However, as the actual nutation frequency deviates from the damper natural frequency (due to spin rate variations and mass property changes due to propellant usage), the dampers experience a significant reduction in effectiveness, an effect characteristic of all tuned passive mechanical systems. Thus, rotor spin rate control must be employed to insure that the damper performance dominates the fuel slosh throughout the mission.

In order to assure acquisition in the presence of a large nutation transient (beyond the dynamic range of the dampers) a second, backup technique, using the axial thrusters, is incorporated into the COMSTAR stabilization system. The Active Nutation Control (ANC) system (described in Ref. 10) utilizes a simple linear accelerometer mounted to the periphery of the rotor to sense nutation. With the accelerometer sensitive axis parallel to the spacecraft spin axis, its output will be a sinusoid at rotor nutation frequency [$\Omega_n = (\sigma - 1)\omega_s$, with $\omega_p = 0$] whose amplitude is proportional to the nutation angle. By using this signal as the command to an axial thruster, the thruster can be fired with the proper

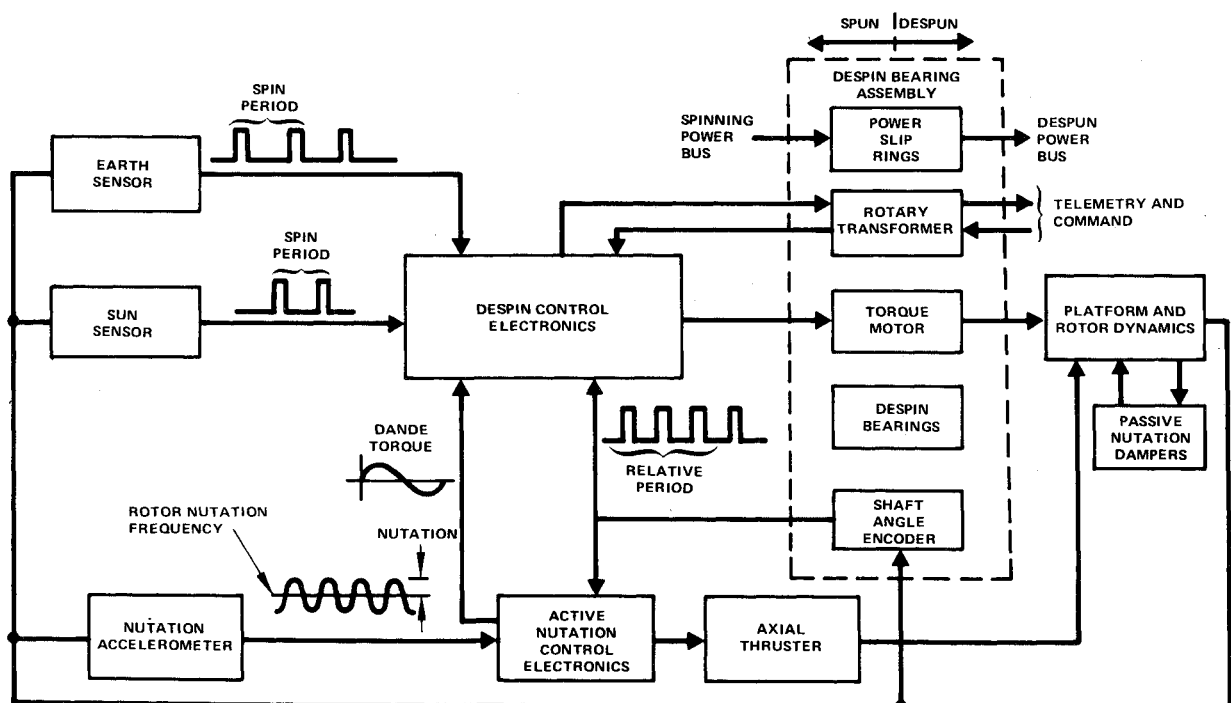


Fig. 1 COMSTAR attitude stabilization and despin control subsystem.

phasing to provide a torque acting to remove the nutation. The ANC will bring the nutation amplitude down to a fixed threshold from an arbitrary initial value after which the passive dampers provide damping for final acquisition.

The second portion of the COMSTAR ADCS is the platform Despin Control Subsystem (DCS), also contained in the spinning rotor. The DCS utilizes inertial rotor phase and rate data provided by the Sun and Earth sensors in conjunction with relative (rotor-to-platform) phase and rate data provided by a shaft-angle-encoder (contained within the despin bearing assembly) to derive the inertial pointing direction of the platform boresight about the spin axis. The error between the actual line of sight (LOS) and the ground-commanded LOS is shaped to develop proper feedback control commands to the electric torque motor contained within the bearing assembly. Once on-station, the DCS maintains an absolute tracking accuracy of 0.15 deg, 3σ with a short-term pointing stability of <0.05 deg, 3σ .

Late in the development phase of the COMSTAR spacecraft, it was decided to add additional damping capability to the control system. It was desired to increase the system stability margin to protect against unforeseen increases in the strength of the fuel slosh dedamping and also to reduce the potential destabilizing effects in transfer orbit or kinematic nutation feedback through the DCS attitude sensors and despun platform dynamic imbalance. Rather than add a third passive damper to the spacecraft with an added weight penalty of ~ 7 lb, an alternate, more efficient scheme was devised using the inherent coupling between the DCS and spacecraft nutation caused by the significant dynamic imbalance of the despun platform. Since the ANC accelerometer and the DCS were both contained in the spinning rotor, it was proposed to use the nutation amplitude information contained in the accelerometer signal to generate a second command to the torque motor which would be summed with the pointing torque command and which would provide transverse torques acting through the product-of-inertia to damp nutation. Since the accelerometer signal and DCS sensor data inherently contain the necessary spin and nutation frequency and phase data, the active damper can become a very broadband device, minimizing the off-resonance degradation behavior experienced by the passive dampers. In addition, the saturation characteristics of the active damper at large nutation angles retain frequency and phase coherence giving a "graceful (linear) degradation" in performance at large angles, a characteristic not found in the passive dampers (which hit mechanical stops and degrade rapidly at large nutation angles). The implementation and performance characteristics of this active damper (known as the DANDE - Despin Active Nutation Damping Electronics) will be discussed in the following section.

III. Active Damper Performance Analysis

A detailed model of the spacecraft dynamics and the active damper design equations are given in Ref. 9. Here we shall repeat only a minimum of simplified results needed to allow a cohesive description of the COMSTAR design. The linearized spacecraft dynamics, assuming for simplicity a symmetric, balanced rotor and a single platform product of inertia, I_{13} , may be written

$$\dot{\omega}_1 + \lambda_n \omega_2 = (I_{J3}/I_T) \dot{\omega}_3 \quad (1a)$$

$$\dot{\omega}_2 - \lambda_n \omega_1 = 0 \quad (1b)$$

$$\dot{\omega}_3 = (I_{l3}/I_p)\dot{\omega}_l - (I_s/I_p)\dot{\omega}_s \quad (1c)$$

$$\dot{\omega}_s = -T_3/I_s \quad (1d)$$

where $\omega = [\omega_I, \omega_2, \omega_3]^T$ is the despun platform inertial rate with equilibrium state $\omega = 0$, $\lambda_n = (I_s/I_T)\omega_s = \sigma\omega_s$, and I_s , I_p , I_T are, respectively, the rotor and platform spin inertias, and

the total spacecraft transverse inertia. T_3 is the internal torque applied by the despin motor, $\dot{\omega}_s$ is the rotor acceleration, and ω_s is the nominal rotor spin speed.

Substituting Eq. (1d) into Eq. (1c) and transforming Eqs. (1a-1c), one obtains

$$\omega = PT \quad (2)$$

where P is the matrix of plant dynamics whose third column of interest here is represented in block diagram form in Fig. 2. Feedback torques to the despin motor are introduced by letting $T = T_b + T_e$ with

$$T_b = -G\omega = - \begin{bmatrix} 0 & 0 & 0 \\ 0 & 0 & 0 \\ K_1 & K_2 & I_n s H(s) \end{bmatrix} \omega \quad (3)$$

which then yields the closed-loop rate equation

$$\omega = [I + PG]^{-1} PT_e = [I + L]^{-1} PT_e \quad (4)$$

The feedback elements are also depicted on Fig. 2. $H(s)$ represents the east-west pointing control open-loop transmission excluding the undamped nutation dipole Q , and is defined in this manner for analytical convenience. The system poles, and in particular the underdamped nutation root, are obtained as the zeroes of the determinant of the return different matrix, i.e.,

$$|I+L| = I + P_{13}K_1 + P_{23}K_2 + P_{33}I_n sH(s) \quad (5)$$

In the active damper implementation, a rotor-mounted accelerometer is used as sensor, which does not directly sense platform rates as indicated by Fig. 2. Instead, the accelerometer senses a linear combination of nutation rates and accelerations in rotor coordinates. The nutation transverse rate feedback path is shown by Fig. 3 from sensor to despin torque command. Nutation sensed by the accelerometer is sinusoidal at rotor nutation frequency $\Omega_n = (\sigma - I)\omega_s = \lambda_n - \omega_s$, while damping torques applied by the despin motor must be at platform (inertial) nutation frequency, λ_n . The required transformation is accomplished by a modulation (frequency shift) using a rotor to platform shaft angle encoder to provide the required coherent relative rate and phase reference. Reduction of the sensed acceleration yields values

$$K_l = -Kr_\rho(2-\sigma)\omega_s \cos\phi' \quad (6a)$$

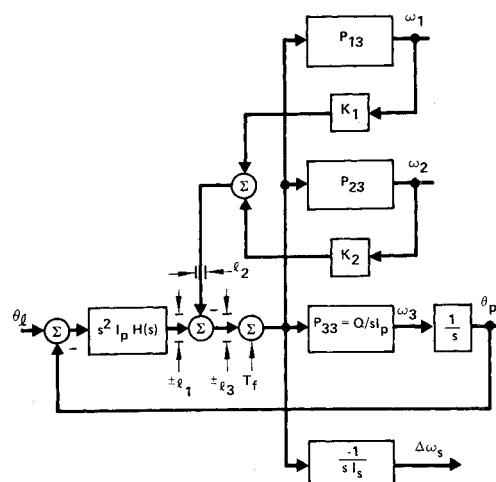


Fig. 2 System diagram of three-axis vehicle dynamics with internal three-axis torque.

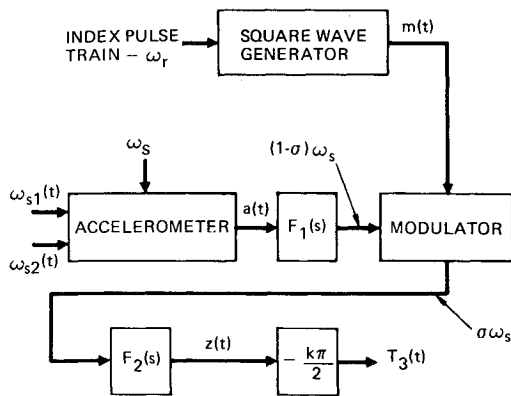


Fig. 3 Nutation sensing and frequency translation mechanization.

$$K_2 = -Kr_0(2-\sigma)\omega_s \sin\phi' \quad (6b)$$

for the transverse rate feedback gains valid for sinusoidal rates, viz., nutation. ϕ' is the phase shift induced by relative accelerometer to index pulse position and the two filters shown on Fig. 3, and K includes the effect of filter gains. Substitution of Eq. (6) in Eq. (5) and extraction of the underdamped nutation root by a root perturbation technique detailed in Ref. 9, the nutation damping constant is ap-

proximated as

$$\tau_d = \frac{-\tau_n [1 + \beta^2 + 2\beta \cos\theta]}{\beta \sin\theta + (K_n \beta / r) \cos(\theta + \phi) + (K_n / r) \cos\phi} \quad (7a)$$

where

$$r = I_{13}^2 / I_p I_T \quad (7b)$$

$$\tau_n = 2 / r \lambda_n \quad (7c)$$

In Eq. (7a), $H(j\lambda_n) = \beta e^{j\theta}$ is the despin pointing loop transmission evaluated at nutation frequency and $K_n = Kr_0(2-\sigma)I_{13}/I_p I_T$, ϕ are the total gain and phase of the transverse rate path. ϕ has contributions due to accelerometer location, product of inertia location, shaft angle encoder phase, and the filters shown in Fig. 3. It is observed in Eq. (7a) that the nutation damping time constant is completely defined by gain and phase parameters at nutation frequency of the two feedback loops.

A sketch of the general active damper design approach is as follows. First, the despin control loop is synthesized by standard techniques to meet despin control transient response and noise and disturbance rejection requirements. This step tends to fix β and θ within limited bounds. τ_d is then approximately proportional to gain K_n and exhibits a minimum with respect to ϕ . ϕ is chosen at the minimizing value, and

Table 1 COMSTAR active damper system parameters and performance characteristics

Parameter/characteristic	Symbol	Value
Rotor spin rate (design range)	ω_s	45–75 rpm (50 rpm nominal)
Transverse inertia over mission	I_T	1080 to 650 slug-ft ²
Despun payload inertia	I_p	127 slug-ft ²
Despun payload product of inertia	I_{23}	31 slug-ft ²
Vehicle inertia ratio over mission	σ	0.22 to 0.28
Accelerometer radius	r_0	3.25 ft
Accelerometer filters	$F_1(s)$	$\frac{978s}{(s+0.42)(s+10)(s+90)}$
	$F_2(s)$	$\frac{4.76}{(s+1.69)[s^2+2(0.5)(1.63)s+(1.63)^2]}$
Despin loop transmission	$H(s)$	$\frac{3 \times 10^3}{I_p(\omega_s - \omega_p)} \left[\frac{1 - e^{-sT}}{s} \right] \left[\frac{(s+0.01)(s+0.33)}{s^3[(s+10)(s+20)]} \right]$
Nutation feedback gain (nominal)	K	6.15 ft-lb/ft/s ² (3.75 ft-lb/deg @ 50 rpm)
Net phase angle (nominal)	θ	–180 deg.
Pointing disturbance	θ_p/θ_n	1.2:1
Dynamic range		0.13 deg of nutation
Nominal damping time constant ($\omega_p = 0$)	τ_d	20 s (one motor on) 12 s (both motors on)

Table 2 COMSTAR nutation time constants – initial synchronous orbit

Number motors	ω_{s0} , rpm	ω_p , rmp	θ , deg	β	K , lb-s ²	ϕ , deg	τ_d , s Eq. (7a)	τ_d , s analog simulation
1	51	0	–159	0.305	6.16	–171	22	23
2				0.61	12.3		8	10
1	70	0	–160	0.214	4.87	–152	28	32
2				0.428	9.75		10	12
1	51	0	–172	0.207	6.16		25	26
2				0.415	12.3	–171	9	7
1	70	0	–172	0.11	3.5		48	59
2				0.22	7.0	–136	20	29

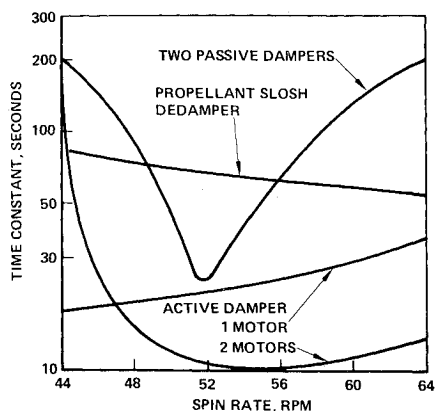


Fig. 4 Active and passive damper performance vs spin rate.

then K_n is adjusted to an appropriate compromise among 1) nutational stability margin, 2) despin pointing disturbances induced during nutation damping, and 3) damper linear operating range.

A summary of applicable COMSTAR system parameters is provided in Table 1. Since the active damper was an add-on experiment on COMSTAR, some restrictions were imposed by the existing spacecraft design. For example, the rotor to platform index pulse phasing, a primary design parameter, had been fixed. Acceptable phasing of the accelerometer feedback was instead achieved electronically with F_2 of Fig. 3. The active damper time constant is shown as a function of spin speed on Fig. 4, along with the dedamper due to propellant slosh which must be stabilized. Also shown is the combined time constant of the two platform-mounted pendulous mechanical dampers. Observe the high degree of tuning associated with the mechanical dampers in contrast to the active damper. Table 2 shows a comparison of predicted active damper time constants obtained from the expression in Eq. (7a) and from a mixed analog simulation of the COMSTAR control system. Agreement is good among these values, and flight data later confirmed these ground predictions.

As well as being broadly tuned, another significant advantage of the despin active damper is its benign degradation in saturation. The point of saturation is the motor torque command which approaches a square wave at platform nutation frequency. The fundamental harmonic of this signal continues to damp nutation, and describing function theory yields a time constant which increases approximately proportional to nutation angle. Such nonlinear behavior has been confirmed by analog simulation and flight data.

IV. Flight Performance

The first COMSTAR spacecraft was launched on May 13, 1976, with the second launched on July 22, 1976. During both transfer orbit and following injection into synchronous orbit, experiments were conducted to measure the performance capability of the active damper. Results from two of these tests illustrating the performance are given in Figs. 5 and 6, showing received spacecraft telemetry signals during the damping tests.

The spacecraft response during the first test of the DANDE in transfer orbit is shown in Fig. 5. The figure shows the time history of the DCS pointing error measurement and the output of the nutation accelerometer. For this test, nutation is induced by pulsed firing of one axial thruster. Without the DANDE enabled, the combined effects of the passive damper (operating off-resonance) and the fuel slosh dedamper give a net nutation damping time constant of ~ 200 s. When the active damper is enabled, the torque applied to the platform causes an immediate response from the DCS with an induced sinusoidal pointing error at platform nutation frequency. With the DANDE now operating, a sevenfold increase in damping is achieved, giving a net decay time constant of 29 s.

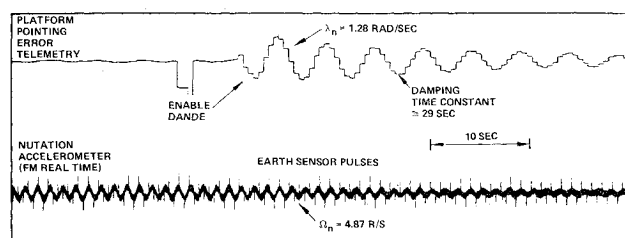
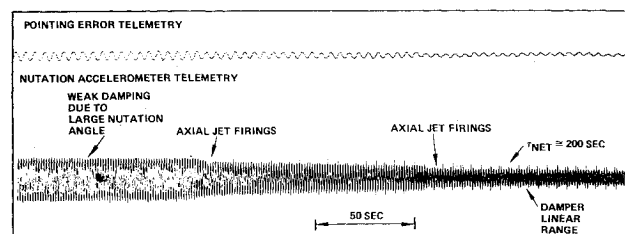
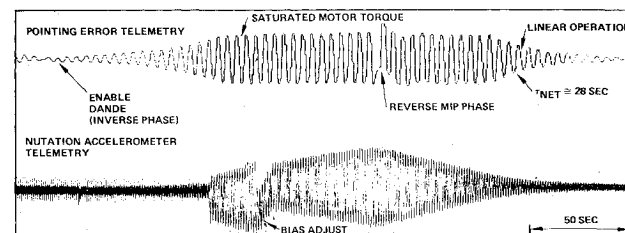


Fig. 5 COMSTAR on-orbit testing 1—initial DANDE checkout (transfer orbit).



a)



b)

Fig. 6 COMSTAR on-orbit testing 2—damping performance comparison (passive vs active).

A second series of tests was conducted to exercise the DANDE at large nutation angles and to compare this with the passive damper performance. The results of these tests are shown in the telemetry time histories in Fig. 6. Figure 6a shows the spacecraft response at a sufficiently large induced nutation angle to exceed the passive damper linear range. The first segment of the tests shows approximately neutral stability with essentially no change seen in the nutation amplitude. The nutation is then reduced in stages by ground firing of an axial thruster until the damper linear range is reached, resulting in a net damping time constant of 200 s. In the second experiment, shown in Fig. 6b, the DANDE is used to induce nutation (through use of a commandable phase reversal built into the electronics) to an amplitude exceeding the DANDE linear range (0.1 deg). When an angle of ~ 0.6 deg is reached, the phase of the DANDE torque is reversed and the nutation immediately begins to decay. As can be seen in the figure, for a saturated DANDE, the nutation converges at a linear rate until the 0.1-deg linear range is reached. At this time, normal exponential decay develops with a net time constant of 28 s.

These results can be compared to the predicted performance obtained from prelaunch analysis and simulations (discussed in Sec. III). The nominal DANDE performance in transfer orbit, at a spin rate of 59 rpm, and with a combined passive damper/fuel slosh dedamper time constant of 200 s, was predicted to be a 25-s decay rate, lower than the 29 s measured. During later experiments conducted with the spacecraft, it was found that the actual product of inertia of the platform was 28 slug-ft² lower than the original, analytically derived POI of 31 slug-ft². Since the DANDE performance is linearly related to the POI (given a fixed damper design), the predicted performance, based on the

reduced POI, should have been 28 s within ~4% of the measured value and well within the time constant measurement uncertainties. Tests performed later in the mission and similar in-orbit testing performed with the second COMSTAR spacecraft yielded additional data which verified both the active damper concept and its performance capabilities.

Some east-west pointing degradation is accepted as a penalty of the active damper during nutation transients. This is evident on Figs. 5 and 6. For COMSTAR the coupling (the ratio between platform azimuth motion and nutation angle) is nominally 1.2:1 (Table 1). However, when no maneuvers are in progress, nutation is asymptotically driven to zero and the pointing effect vanished likewise.

V. Concluding Remarks

This paper has described the design, implementation, and in-orbit performance of a new technique for stabilization of dual-spin satellites developed for and flown on the COMSTAR spacecraft. The control scheme makes use of the inherent coupling between the payload pointing control system and vehicle nutation, through a payload dynamic imbalance, to provide a substantial active nutation control capability. Experience gained with the development and in-flight operation of the COMSTAR active damper has shown the technique to be a highly effective and efficient method of obtaining significant nutation control with minimal complexity and cost. Significant weight and performance advantages are realized over equivalent passive damping techniques. The success of the COMSTAR DANDE experiment has led to consideration of deletion of all passive

damping mechanisms from the attitude control system of future spacecraft, with significant weight and cost savings, along with elimination of potentially undesirable constraints on the ground operation of these spacecraft.

References

- ¹Iorillo, A.J., "Analysis Related to the Hughes Gyrostat System," Hughes Aircraft Co., Rept. SSST0438B, Dec. 1967.
- ²Likins, P.W., "Attitude Stability Criteria for a Dual-Spin Spacecraft," *Journal of Spacecraft and Rockets*, Vol. 4, April 1967, pp. 1638-1643.
- ³Mingori, D.L., "Effects of Energy Dissipation on the Attitude Stability of Dual-Spin Satellites," *AIAA Journal*, Vol. 7, Jan. 1969, pp. 20-27.
- ⁴Neer, J.T., "Intelsat IV Nutation Dynamics," AIAA Paper 72-537, Washington, D.C., April 1972.
- ⁵Phillips, K.J., "Active Nutation Damping Utilizing Spacecraft Mass Properties," *IEEE Transactions on Aerospace and Electronic Systems*, Vol. AES-9, Sept. 1973.
- ⁶Phillips, K.J., "Linearization of the Closed-Loop Dynamics of a Dual-Spin Spacecraft," *Journal of Spacecraft and Rockets*, Vol. 8, Sept. 1971, pp. 938-944.
- ⁷Leliakov, I.P. and Barba, P.M., "Damping Spacecraft Nutation by Means of a Despun Antenna," *AAS/AIAA Astrodynamics Conference*, Vail, Colorado, 1973.
- ⁸Slafér, L.I. and Marbach, H.D., "Active Control of the Dynamics of a Dual-Spin Spacecraft," *Journal of Spacecraft and Rockets*, Vol. 12, May 1975, pp. 287-293.
- ⁹Smay, J.W. and Slafér, L.I., "Dual-Spin Spacecraft Stabilization using Nutation Feedback and Inertia Coupling," *Journal of Spacecraft and Rockets*, Vol. 13, Nov. 1976, pp. 650-659.
- ¹⁰Grasshoff, L.H., "An Onboard, Closed-Loop, Nutation Control System for a Spin Stabilized Spacecraft," *Journal of Spacecraft and Rockets*, Vol. 5, May 1968, pp. 530-535.

From the AIAA Progress in Astronautics and Aeronautics Series . . .

TURBULENT COMBUSTION—v. 58

Edited by Lawrence A. Kennedy, State University of New York at Buffalo

Practical combustion systems are almost all based on turbulent combustion, as distinct from the more elementary processes (more academically appealing) of laminar or even stationary combustion. A practical combustor, whether employed in a power generating plant, in an automobile engine, in an aircraft jet engine, or whatever, requires a large and fast mass flow or throughput in order to meet useful specifications. The impetus for the study of turbulent combustion is therefore strong.

In spite of this, our understanding of turbulent combustion processes, that is, more specifically the interplay of fast oxidative chemical reactions, strong transport fluxes of heat and mass, and intense fluid-mechanical turbulence, is still incomplete. In the last few years, two strong forces have emerged that now compel research scientists to attack the subject of turbulent combustion anew. One is the development of novel instrumental techniques that permit rather precise nonintrusive measurement of reactant concentrations, turbulent velocity fluctuations, temperatures, etc., generally by optical means using laser beams. The other is the compelling demand to solve hitherto bypassed problems such as identifying the mechanisms responsible for the production of the minor compounds labeled pollutants and discovering ways to reduce such emissions.

This new climate of research in turbulent combustion and the availability of new results led to the Symposium from which this book is derived. Anyone interested in the modern science of combustion will find this book a rewarding source of information.

485 pp., 6 × 9, illus. \$20.00 Mem. \$35.00 List

TO ORDER WRITE: Publications Dept., AIAA, 1290 Avenue of the Americas, New York, N. Y. 10019